HHS Public Access

Author manuscript

Neuroscience. Author manuscript; available in PMC 2016 December 03.

Published in final edited form as:

Neuroscience. 2015 December 3; 310: 188–197. doi:10.1016/j.neuroscience.2015.09.016.

Progressive irreversible hearing loss is caused by stria vascularis degeneration in an *Slc26a4*-insufficient mouse model of large vestibular aqueduct syndrome

Taku Ito[a,*], **Ayako Nishio**[a,*], **Philine Wangemann**[b], and **Andrew J. Griffith**[a]

[a]Otolaryngology Branch, National Institute on Deafness and Other Communication Disorders, National Institutes of Health, Bethesda, Maryland, USA, 20892

[b]Anatomy and Physiology Department, Kansas State University, Manhattan, Kansas, USA, 66506

Abstract

Hearing loss of patients with enlargement of the vestibular aqueduct (EVA) can fluctuate or progress, with overall downward progression. The most common detectable cause of EVA is mutations of *SLC26A4*. We previously described a transgenic *Slc26a4*-insufficient mouse model of EVA in which *Slc26a4* expression is controlled by doxycycline administration. Mice that received doxycycline from conception until embryonic day 17.5 (DE17.5) had fluctuating hearing loss between 1 and 6 months of age with an overall downward progression after 6 months of age. In this study, we characterized the cochlear functional and structural changes underlying irreversible hearing loss in DE17.5 mice at 12 months of age. The endocochlear potential was decreased and inversely correlated with auditory brainstem response thresholds. The stria vascularis was thickened and edematous in ears with less severe hearing loss, and thinned and atrophic in ears with more severe hearing loss. There were pathologic changes in marginal cell morphology and gene expression that were not observed at 3 months. We conclude that strial dysfunction and degeneration is the primary cause of irreversible progressive hearing loss in our *Slc26a4*-insufficient mouse model of EVA. This model of primary strial atrophy may be used to explore the mechanisms of progressive hearing loss due to strial dysfunction.

Keywords

deafness; DFNB4; doxycycline; fluctuation; hypomorphic; pendrin; presbycusis; *SLC26A4*; stria vascularis

Address correspondence to: Andrew J. Griffith, Otolaryngology Branch, National Institute on Deafness and Other Communication Disorders, National Institutes of Health, 35A Convent Drive, Room GF-103, Bethesda, Maryland 20892-3729, USA. Phone: 301.402.2829; Fax: 301.402.7580; griffita@nidcd.nih.gov.

*contributed equally to this study and manuscript.

Introduction

Enlargement of the vestibular aqueduct (EVA; OMIM 600791) is the most commonly detected radiological malformation in children with sensorineural hearing loss (SNHL) (Morton and Nance 2006). Patients with EVA have hearing loss that can fluctuate or progress incrementally and thought to result in overall downward progression (Jackler and De La Cruz 1989, Levenson, Parisier et al. 1989, Griffith and Wangemann 2011). The most common detectable cause of EVA is mutations affecting the exonic or adjacent splice site sequences of the *SLC26A4* gene (OMIM 605646) (Everett, Glaser et al. 1997). *SLC26A4* encodes a multi-pass transmembrane protein called pendrin (Everett, Glaser et al. 1997). Approximately 1/4 of North American and European Caucasian EVA patients have two detectable mutant alleles of *SLC26A4*, 1/4 have one detectable mutant allele, and 1/2 have no obvious mutations in the coding region of this gene (Campbell, Cucci et al. 2001, Choi, Stewart et al. 2009).

Pendrin is an anion-base exchanger expressed in a subset of organs that includes the inner ear, thyroid, and kidney (Everett, Glaser et al. 1997). In the mouse inner ear, pendrin is expressed in nonsensory epithelial cells of the cochlear duct, vestibular organs, and endolymphatic sac (Royaux, Belyantseva et al. 2003). Mice that are homozygous for a targeted deletion allele (*Slc26a*$^{\Delta}$) of *Slc26a4* have profound hearing loss, vestibular dysfunction, and massively enlarged endolymphatic spaces throughout the entire inner ear (Everett, Belyantseva et al. 2001). A series of studies of *Slc26a*$^{\Delta/\Delta}$ mice revealed numerous pathologic changes that include enlargement of all of the endolymph-containing compartments (Everett, Belyantseva et al. 2001, Kim and Wangemann 2010), endolymph acidification (Nakaya, Harbidge et al. 2007, Wangemann, Nakaya et al. 2007, Kim and Wangemann 2011), oxidative stress and loss of KCNJ10 expression in stria vascularis (Singh and Wangemann 2008), loss of the endocochlear potential (EP) (Royaux, Belyantseva et al. 2003, Wangemann, Itza et al. 2004), followed by macrophage invasion, degeneration and hyperpigmentation of stria vascularis (Wangemann, Itza et al. 2004, Jabba, Oelke et al. 2006). *Slc26a*$^{\Delta/\Delta}$ mice fail to acquire normal hearing at postnatal day 12 and therefore the mechanisms of fluctuating and progressive hearing loss could not be explored in this model.

In order to further characterize the pathogenesis of hearing loss caused by *Slc26a4* insufficiency, we developed a doxycycline-inducible *Slc26a4* mouse model that utilizes genetically unlinked effector (Tg[E]) and responder (Tg[R]) transgenes to express pendrin in the presence, but not absence, of doxycycline (Choi, Kim et al. 2011). The transgenes were crossed onto the *Slc26a*$^{\Delta/\Delta}$ background so that all pendrin expression is derived from the responder transgene. We showed that *Slc26a4* expression is only required from E16.5 to P2 for the acquisition of normal hearing at one month of age (Choi, Kim et al. 2011). Li et al. (Li, Sanneman et al. 2013) used a different rescue strategy to demonstrate that pendrin must be expressed in the endolymphatic sac, but not the cochlea, to rescue normal inner ear function in *Slc26a4*$^{\Delta/\Delta}$ mice. These studies collectively indicated that *Slc26a4* expression is required in the endolymphatic sac from E16.5 to P2 for the initial acquisition of normal hearing.

In order to determine if *Slc26a4* expression is required to maintain hearing in *Slc26a4*-insufficient ears, we manipulated pendrin expression in Tg[E];Tg[R]; *Slc26a4*$^{\Delta/\Delta}$ mice through various paradigms of doxycycline administration. Some paradigms resulted in mice with unilateral or asymmetric hearing loss (Choi, Kim et al. 2011). This phenotype closely models the hearing loss associated with EVA in humans, which is typically unilateral or asymmetric (Jackler and De La Cruz 1989, Levenson, Parisier et al. 1989, Griffith and Wangemann 2011). We characterized the natural history and pathogenesis of hearing loss after one month of age in Tg[E];Tg[R]; *Slc26a*$^{\Delta/\Delta}$ mice which received doxycycline from conception until E17.5 (DE17.5) (Ito, Li et al. 2014). The mice had fluctuating hearing loss between 1 and 6 months of age with an overall downward progression after 6 months of age. The fluctuating hearing loss was correlated with pathologic changes of the stria vascularis and loss of the endocochlear potential (Ito, Li et al. 2014). The DE17.5 mice had no visible abnormalities or loss of hair cells or spiral ganglion neurons, but their striae vascularis showed numerous pathologic changes including hyperpigmentation, loss of the KCNJ10 protein which is required to generate the EP, swelling, and degeneration of intermediate and marginal cells (Ito, Li et al. 2014). The DE17.5 striae also showed increased levels of mRNA encoding macrophage marker proteins and increased staining of macrophages that could reflect macrophage proliferation, recruitment or activation (Ito, Li et al. 2014). The ability to recover hearing progressively declined until it appeared to be completely and irreversibly lost after 6 months of age (Ito, Li et al. 2014). In the present study, we characterized the cochlear functional and structural changes that underlie this irreversible progressive hearing loss in the DE17.5 mice at 12 months of age.

Materials and Methods

Ethics Statement

All animal experiments and procedures were performed according to protocols approved by the Animal Care and Use Committee of the National Institute of Neurological Diseases and Stroke and the National Institute on Deafness and Other Communication Disorders, National Institutes of Health.

Animals

The effector transgene (Tg[E]; Tg(RP23-265L9/rtTA2S-M2/NeoR)1Ajg) and the responder transgene (Tg[R]; Tg(AcGFP/TRE/Slc26a4)2Ajg) were expressed in *Slc26a4*$^{\Delta/\Delta}$ and *Slc26a4*$^{\Delta/+}$ mice. Transgenes and their background strain history have been described (Choi, Kim et al. 2011, Ito, Li et al. 2014). We defined Tg[E];Tg[R];*Slc26a4*$^{\Delta/\Delta}$ mice as experimental animals and Tg[E];Tg[R];*Slc26a4*$^{\Delta/+}$ littermates or offspring of the same parents as control animals. Experimental and control animals were administered doxycycline from conception until E17.5. Doxycycline was administered in drinking water containing 0.2 g doxycycline hyclate (Sigma-Aldrich) and 5 g sucrose (MP Biomedicals) per 100 ml of reagent-grade water (Choi, Kim et al. 2011, Ito, Li et al. 2014). Doxycycline-containing water was provided to the dam from the onset of mating and substituted with doxycycline-free water at embryonic day 17.5 as described (Choi, Kim et al. 2011, Ito, Li et al. 2014).

Genotype analysis

Genomic DNA was isolated and analyzed by polymerase chain reaction (PCR) for the presence of the effector transgene (Tg[E]), the responder transgene (Tg[R]), and the alleles *Slc26a4*$^{\Delta}$ and *Slc26a4*$^{+}$ as described (Choi, Kim et al. 2011, Ito, Li et al. 2014).

Endocochlear potential

The endocochlear potential (EP) was measured and recorded as described (Choi, Kim et al. 2011, Ito, Li et al. 2014). A round-window approach through the basilar membrane of the first turn of the cochlea was used to measure the endocochlear potential in the basal turn of the cochlea (Wangemann, Itza et al. 2004, Wangemann, Nakaya et al. 2007, Ito, Li et al. 2014). For measurement of anoxic EP, anoxia was induced by intramuscular injection of succinylcholine chloride (0.1 μg/g) after establishment of deep anesthesia. Anoxia interferes with oxidative metabolism and ATP generation necessary for active transport and generation of the positive EP by stria vascularis (Thalmann, Miyoshi et al. 1972). Thus, the magnitude of the EP at normoxic conditions reflects the function of the stria vascularis. Within a few minutes of anoxia, however, the EP declines from a normal positive potential of 80 to 100 mV to a negative potential of approximately −30 to −40 mV (Johnstone 1965). This negative potential reflects activity of the organ of Corti. It depends on open transduction channels in apical membranes and open K^+ channels in basolateral membranes (Asakuma, Lowry et al. 1979, Marcus 1984). The magnitude of the negative EP is an indirect indicator of hair cell function.

Auditory brainstem response thresholds

Auditory brainstem response (ABR) thresholds for click stimuli were measured as described (Ito, Li et al. 2014). If an ear had no detectable waveform in response to the highest intensity level of 120 dB sound pressure level (SPL), the threshold was considered to be 125 dB SPL for subsequent analyses. Hearing thresholds < 45 dB SPL were considered normal. Thresholds ≥ 45 dB SPL and ≥ 80 dB SPL were defined as moderate and severe hearing loss, respectively. Wave I amplitudes were not measured at the time of initial data collection. The original waveform tracings were not backed up in electronic files and could not be located for retrospective analysis.

Histopathology

Mice were euthanized by CO_2 exposure followed by cervical dislocation. Inner ears were dissected and tissue sections prepared and stained as described (Choi, Kim et al. 2011, Ito, Li et al. 2014). Five regions were analyzed in each ear. Each region was comprised of four contiguous midmodiolar sections that were examined to identify a section with maximal tissue preservation that was used for quantitative analysis. Five regions and sections representing a total specimen thickness of 80 μm were analyzed per animal. Each tissue section contained apical, middle and basal turns of cochlea. The distance from the apex was approximately 20%, 45% and 80%, respectively, for the regions of the apical, middle and basal turns that were analyzed. These locations approximately correspond to 8 kHz, 16 kHz and 48 kHz, respectively, on the place-frequency map of the mouse cochlea (Viberg and Canlon 2004). Images were captured for measurements of stria vascularis thickness, spiral

ganglion cell density, inner hair cell survival rate, and outer hair cell survival rate as described (Ito, Li et al. 2014). Spiral ganglion cell density was measured within Rosenthal's canal.

Immunohistochemistry

Whole-mounted and sectioned mouse cochleae were immunostained for KCNJ10 or KCNQ1 and visualized as described (Ito, Li et al. 2014). Rabbit anti-KCNJ10 antibodies (Alomone, Jerusalem, Israel) were diluted 1:300 or goat anti-KCNQ1 antibodies (Santa Cruz Biotechnology, Santa Cruz, CA) were diluted 1:200 in blocking solution. Secondary antibodies were donkey anti-goat IgG conjugated with FITC (Santa Cruz Biotechnology) or goat anti-rabbit IgG conjugated with Alexa Fluor 568 (Invitrogen, Carlsbad, CA) diluted 1:500. Whole-mount samples were counterstained with rhodamine-phalloidin (Molecular Probes, Eugene, OR) diluted 1:100. Apical surface areas of marginal cells of striae vascularis were measured using Image J software (National Institutes of Health).

Quantitative RT-PCR

The lateral wall was excised from at least 5 cochleae with each genotype at 12 months of age. mRNA was extracted and quality was confirmed using an Agilent Bioanalyzer (Agilent Technologies). mRNA was reverse transcribed into cDNA for qPCR analysis with efficient primer sets specific to *Actb*, *Cd68*, *Lyz2* or *Cd45* with ZEN double-quenched probes containing a 5′ FAM fluorophore, 3′ IBFQ quencher, and an internal ZEN quencher (IDT, Coralville, IA). Sequences for primers and probes are: 5′-AGGTCTTTACGGATGTCAACG-3′, 5′-TCACTATTGGCAACGAGCG-3′ and 5′-AAAAGAGCC/ZEN/TCAGGGCATCGGAA-3 for *Actb;* 5′-GTGTCTGATCTTGCTAGGACC-3′, 5′-TGTGCTTTCTGTGGCTGTAG-3′ and 5′-TGAAGGATG/ZEN/GCAGGAGAGTAACGG-3 for *Cd68*; 5′-CAAAGAGGGTGGTGAGAGATC-3′, 5′-TGAGAAAGAGACCGAATGAGC-3′ and 5′-TTTTGACAG/ZEN/TGTGCTCGCCATGC-3 for *Lyz2*; 5′-GACAGAGTTAGTGAATGGAGACC-3′, 5′-AAAAGTTCGGAGAGTGTAGGC-3′ and 5′-TCTGCTTTC/ZEN/CTTCGCCCCAGT-3 for *Cd45*. Comparative TaqMan® assays were performed on an ABI 7500 real-time PCR system (Applied Biosystems). PCR reactions were performed in a 10-μl volume containing 2 μl cDNA, 1 μl primer mix (IDT), 5 μl of Universal PCR Master Mix (Applied Biosystems) and 2 μl water. Cycling conditions were 50°C for 2 min, 95°C for 10 min, followed by 40 cycles of 15 s at 95°C and 1 min at 60°C. Relative expression was normalized to the level of β-actin expression (encoded by *Actb*), and calculated as $2^{-\Delta\Delta CT}$ using the comparative threshold cycle method (Ito, Li et al. 2014).

Statistics

Statistical analyses included Pearson correlation, Student's *t* test and one-way ANOVA. A Tukey post hoc test was performed when significant differences were detected by one-way ANOVA. $p < 0.05$ was considered to be significant. Pearson correlations were described as: (1) strong if $-1.0 \leq R \leq -0.5$ or $0.5 \leq R \leq 1.0$; (2) moderate if $-0.5 < R < -0.3$ or $0.3 < R < 0.5$; or (3) weak if $-0.3 \leq R \leq 0.1$ or $0.1 \leq R \leq 0.3$.

Results

Endocochlear Potential

We hypothesized that progressive hearing loss in DE17.5 experimental mice at 12 months of age is caused by reduction of the EP. The mean EP in control ears at 12 months of age was 98.9 mV (n=12; Fig. 1A). This value was indistinguishable from those we previously reported for control ears at 1 and 3 months of age: 98.1 mV and 99.4 mV, respectively (Ito, Li et al. 2014). In contrast, the mean EP in experimental ears at 12 months of age was significantly decreased (Tukey post hoc test, $p < 0.05$) at 46.0 mV (Fig. 1A) in comparison to values that we previously reported for experimental ears at 1 and 3 month of age: 63.4 mV and 63.6 mV, respectively (Ito, Li et al. 2014). There was a strong negative correlation of EP values with click ABR thresholds measured at 12 months of age ($R = -0.74$, $p < 0.001$) (Fig. 1B). These results implicate reduction of the EP as the cause of irreversible progression of hearing loss in DE17.5 experimental mice at 12 months of age.

In addition to measurements of the EP at normoxic conditions, we measured the EP under anoxic conditions. The magnitude of the negative anoxic EP is an indirect indicator of hair cell function. The anoxic EPs of experimental ears were not correlated ($p=0.17$) with click ABR thresholds (Fig. 1C). This result may suggest that loss of hair cell function is not the primary cause of progression of hearing loss in DE17.5 mice. Alternatively, it could reflect inadequate statistical power to detect a correlation due to the low number (n=7) of experimental measurements (Fig. 1C).

Cochlear duct histomorphology

To identify histopathologic changes that could account for the reduction of the normal and anoxic EP, we used light microscopy to quantitatively evaluate cochleae at 12 months of age (Fig. 2). The mean spiral ganglion cell density in experimental ears was not different from that of control ears at the apical or basal turns ($p = 0.95$ or $p = 0.57$, respectively), but was different at the middle turns ($p = 0.03$) (Fig. 3A). Spiral ganglion cell densities were not correlated with click ABR thresholds in the apical, middle, or basal turns of experimental ears ($R = 0.10$, $p = 0.80$; $R = 016$, $p = 0.67$; and $R = 0.32$, $p = 0.43$, respectively) (Fig. 5A, Table 1). This result suggests that loss of spiral ganglion neurons is not the cause of progression of hearing loss in DE17.5 mice.

Survival rates of inner hair cells in the apical, middle, and basal turns of experimental ears were not different from those of control ears ($p = 0.18$, $p = 0.05$, and $p = 0.19$, respectively) (Fig. 3B). In contrast, survival rates of outer hair cells in the apical, middle, and basal turns of experimental ears were moderately but significantly lower than those of control ears ($p = 0.003$, $p = 0.0004$, and $p = 0.0005$, respectively) (Fig. 3C). The outer hair cell survival rates in the apical and basal turns were not correlated with click ABR thresholds in experimental ears ($R = -0.40$, $p = 0.29$; and $R = -0.33$, $p = 0.38$, respectively), but were strongly correlated in the middle turn ($R = -0.81$, $p = 0.008$) (Fig. 5B, Table 1). This correlation was not different ($p=0.28$) from the corresponding correlation in the ears of control mice, so we cannot reject the null hypothesis that the relationship of outer hair cell survival to click ABR thresholds is the same in both control and experimental ears. Therefore a contribution of loss

of hair cells to loss of hearing in experimental ears cannot be directly attributable to the *Slc26a4* insufficiency.

The thickness of stria vascularis in the apical, middle, and basal turns of experimental ears was not different from that of control ears at ($p = 0.85$, $p = 0.20$, and $p = 0.64$, respectively). However, we observed a greater variability leading to larger standard deviations in experimental ears (Fig. 3D). Upon further analysis, we observed atrophic thinning of the stria vascularis in experimental ears with severe hearing loss (Fig. 2B), and edematous thickened stria vascularis in experimental ears with moderate hearing loss (Fig. 2D). Thickness of stria vascularis in experimental ears with severe hearing loss was less than that in control ears in all cochlear turns ($p=0.00112$, $p=0.00001$, $p=0.00001$) and the thickness of stria vascularis in experimental ears with moderate hearing loss was thicker than that of control ears ($p=0.00057$, $p=0.00248$, $p=0.00001$; Fig. 4). The thickness of the stria vascularis in the apical and middle turns was not correlated with click ABR thresholds in experimental ears ($R = -0.41$, $p = 0.28$; and $R = -0.67$, $p = 0.07$, respectively), but it was correlated in the basal turn ($R = -0.72$, $p = 0.03$) (Fig. 5C, Table 1). These results indicate that reduction of the EP was associated with atrophy of the stria vascularis, at least in the basal turn, of DE17.5 experimental cochleae at 12 months of age.

Stria vascularis architecture

We examined the morphology and the expression of selected proteins in intermediate cells and marginal cells of stria vascularis of DE17.5 control and experimental ears at 12 months of age. Expression of KCNJ10, a K^+ channel protein that is required by intermediate cells to generate the EP, was clearly detected in control ears (Fig. 6A). In contrast, it was present at comparatively low or non-detectable levels in experimental ears (Fig. 6C), consistent with the reduction of EP in those ears. In control ears, the marginal cells had a well-organized cobblestone appearance and a uniform apical surface area (Fig. 6B, 6E). In comparison, the marginal cells in experimental ears were irregular in size and organization at 12 months of age (Fig. 6D, 6F). In the experimental ears, marginal cells were either enlarged and lacking KCNQ1, or they were abnormally small with sustained KCNQ1 expression on their apical surfaces (Fig. 6D, 6F). The abnormally enlarged cells were previously observed in *Slc26a*$^{\Delta/\Delta}$ ears by Jabba et al. (Jabba, Oelke et al. 2006). There were numerous accumulations of pigment granules in the stria vascularis of experimental, but not control, ears (Fig. 6).

The RNA levels of the macrophage marker genes *Cd68*, *Lyz2* and *Cd45* were also elevated in the stria vascularis of experimental ears (Fig. 7). These results collectively implicate the stria vascularis as the primary site of cochlear pathology associated with irreversible progressive hearing loss in the ears of *Slc26a4*-insufficient (DE17.5) mice.

Discussion

We previously characterized the natural history and pathogenesis of hearing loss in an *Slc26a4*-insufficient mouse model (DE17.5 mice) (Ito, Li et al. 2014). The DE17.5 mice had fluctuating hearing loss between 1 and 6 months of age, with overall downward progression observed at 9 and 12 months of age. At 3 months of age, the fluctuating ABR thresholds were correlated with loss of the endocochlear potential (EP) and pathologic changes of the

stria vascularis (Ito, Li et al. 2014). Here we studied the DE17.5 mice at 12 months of age to characterize the cochlear functional and structural correlates of irreversible progressive hearing loss. Our results indicate that irreversible progressive hearing loss in DE17.5 mice is primarily caused by degeneration and loss of function of the stria vascularis.

At 12 months of age, the EP was significantly decreased in experimental ears (Fig. 1A). Strial pathology, either in the form of edema or atrophy, was observed in experimental ears (Fig. 2B, 2D). Thickened and edematous striae vascularis were observed at 3 months of age, but atrophy was not observed at that time point (Ito, Li et al. 2014). In our current study of 12 month-old ears, we observed thickened and edematous striae vascularis in experimental ears with less severe hearing loss (Fig. 2D, 4, 5C) and well-preserved EPs (Fig. 1B). In contrast, we observed atrophy of the striae vascularis in experimental ears with severe hearing loss (Fig. 2B, 4, 5C) and reduced EPs. These findings suggest that the thickened and edematous stria vascularis reflects a reversible structural change associated with reversible hearing loss, whereas the atrophic stria vascularis corresponds to irreversible hearing loss. This sequence of acute strial edema followed by chronic strial atrophy resembles that observed in the stria vascularis of ears exposed to ototoxic levels of noise (Hirose and Liberman 2003). Strial atrophy does not appear to involve apoptosis since TUNEL staining of the stria vascularis of experimental ears was negative (unpublished observation). Phagocytosis of intermediate cells, marginal cells, or both may contribute to these irreversible degenerative changes.

Pathologic heterogeneity in the apical surface area and in the expression of KCNQ1 was observed in marginal cells of experimental ears at 12 months of age (Fig. 6). We did not observe these marginal cell changes at 3 months of age (Ito, Li et al. 2014). Our experimental mice do not show enlargement of endolymphatic spaces at 12 months of age (Fig. 2B, 2D), so the marginal cell expansion is unlikely to be caused by scala media expansion. KCNQ1 is required for normal stria vascularis function (Shen, Marcus et al. 1997, Lang, Vallon et al. 2007) and loss of its expression could contribute to the irreversible loss of hearing at 12 months of age in experimental ears of DE17.5 mice.

The molecular and cellular mechanisms underlying these observations are unclear. What causes these irreversible changes in the structure and function of the stria vascularis in experimental ears? Repeated strial edema may cause cumulative damage to strial function that eventually results in a loss of recovery and progression to strial atrophy. The results of this study and others (Juhn and Rybak 1981, Wangemann, Liu et al. 1995, Wangemann, Itza et al. 2004, Zhang, Dai et al. 2012), suggest that other functional lesions may exist, such as leakiness of the blood-labyrinth barrier, loss of Na/K-ATPase activity in the marginal cells, or loss of KCNJ10 function. The underlying mechanism of irreversible hearing loss may thus be complex and multifactorial.

Stria vascularis atrophy appears to follow the loss of hair cells and spiral ganglion cells in most mouse models of age-related hearing loss. There are only a few reported mouse models with strial atrophy as the primary cause of presbycusis. BALB/cJ mice and C57BL/6-*Tyr*$^{c\text{-}2J}$ mice showed age-related decline of the EP, strial thinning, and loss of strial marginal cells by 19 and 24 months of age, respectively (Ohlemiller, Lett et al. 2006, Ohlemiller 2009,

Ohlemiller, Rice et al. 2009). Our *Slc26a4*-insufficient mice provide a novel model of primary strial atrophy, corresponding to a common monogenic disorder of human hearing. This model may be used to explore the mechanism of progressive loss of hearing due to strial dysfunction. The model may be applicable to more common forms of hearing loss caused by strial dysfunction, such as age-related strial presbycusis. Further studies of *Slc26a4*-insufficient mice may provide insights into potential therapies to modulate or prevent hearing loss associated with EVA, presbycusis or other related disorders.

Acknowledgments

This work was supported by NIH intramural research funds Z01-DC000060 and Z01-DC000080. A.N. was supported in part by a JSPS Research Fellowship for Japanese Biomedical and Behavioral Researchers at NIH. P.W. was supported by NIH grant R01-DC012151. We thank Tracy Fitzgerald and our NIDCD colleagues for helpful suggestions and advice, Ken Kitamura for support, and Inna Belyantseva, Tom Friedman and Mike Hoa for critical reading of the manuscript.

References

Asakuma S, Lowry LD, Snow JB Jr. Effect of kanamycin sulfate on the endocochlear dc potential of guinea pigs. Arch Otolaryngol. 1979; 105(3):145–148. [PubMed: 420653]

Campbell C, Cucci RA, Prasad S, Green GE, Edeal JB, Galer CE, Karniski LP, Sheffield VC, Smith RJ. Pendred syndrome, DFNB4, and PDS/SLC26A4 identification of eight novel mutations and possible genotype-phenotype correlations. Hum Mutat. 2001; 17(5):403–411. [PubMed: 11317356]

Choi BY, Kim HM, Ito T, Lee KY, Li X, Monahan K, Wen Y, Wilson E, Kurima K, Saunders TL, Petralia RS, Wangemann P, Friedman TB, Griffith AJ. Mouse model of enlarged vestibular aqueducts defines temporal requirement of Slc26a4 expression for hearing acquisition. J Clin Invest. 2011; 121(11):4516–4525. [PubMed: 21965328]

Choi BY, Stewart AK, Madeo AC, Pryor SP, Lenhard S, Kittles R, Eisenman D, Kim HJ, Niparko J, Thomsen J, Arnos KS, Nance WE, King KA, Zalewski CK, Brewer CC, Shawker T, Reynolds JC, Butman JA, Karniski LP, Alper SL, Griffith AJ. Hypo-functional SLC26A4 variants associated with nonsyndromic hearing loss and enlargement of the vestibular aqueduct: genotype-phenotype correlation or coincidental polymorphisms? Hum Mutat. 2009; 30(4):599–608. [PubMed: 19204907]

Dallos P. Some electrical circuit properties of the organ of Corti. I. Analysis without reactive elements. Hear Res. 1983; 12(1):89–119. [PubMed: 6319350]

Everett LA I, Belyantseva A, Noben-Trauth K, Cantos R, Chen A, Thakkar SI, Hoogstraten-Miller SL, Kachar B, Wu DK, Green ED. Targeted disruption of mouse Pds provides insight about the inner-ear defects encountered in Pendred syndrome. Hum Mol Genet. 2001; 10(2):153–161. [PubMed: 11152663]

Everett LA, Glaser B, Beck JC, Idol JR, Buchs A, Heyman M, Adawi F, Hazani E, Nassir E, Baxevanis AD, Sheffield VC, Green ED. Pendred syndrome is caused by mutations in a putative sulphate transporter gene (PDS). Nat Genet. 1997; 17(4):411–422. [PubMed: 9398842]

Griffith AJ, Wangemann P. Hearing loss associated with enlargement of the vestibular aqueduct: mechanistic insights from clinical phenotypes, genotypes, and mouse models. Hear Res. 2011; 281(1–2):11–17. [PubMed: 21669267]

Hirose K, Liberman MC. Lateral wall histopathology and endocochlear potential in the noise-damaged mouse cochlea. J Assoc Res Otolaryngol. 2003; 4(3):339–352. [PubMed: 14690052]

Ito T, Li X, Kurima K, Choi BY, Wangemann P, Griffith AJ. Slc26a4-insufficiency causes fluctuating hearing loss and stria vascularis dysfunction. Neurobiol Dis. 2014; 66:53–65. [PubMed: 24561068]

Jabba SV, Oelke A, Singh R, Maganti RJ, Fleming S, Wall SM, Everett LA, Green ED, Wangemann P. Macrophage invasion contributes to degeneration of stria vascularis in Pendred syndrome mouse model. BMC Med. 2006; 4:37. [PubMed: 17187680]

Jackler RK, De La Cruz A. The large vestibular aqueduct syndrome. Laryngoscope. 1989; 99(12): 1238–1242. discussion 1242–1233. [PubMed: 2601537]

Johnstone BM. THE RELATION BETWEEN ENDOLYMPH AND THE ENDOCOCHLEAR POTENTIAL DURING ANOXIA. Acta Otolaryngol. 1965; 60:113–120. [PubMed: 14337946]

Juhn SK, Rybak LP. Labyrinthine barriers and cochlear homeostasis. Acta Otolaryngol. 1981; 91(5–6): 529–534. [PubMed: 6791457]

Kim HM, Wangemann P. Failure of fluid absorption in the endolymphatic sac initiates cochlear enlargement that leads to deafness in mice lacking pendrin expression. PLoS One. 2010; 5(11):e14041. [PubMed: 21103348]

Kim HM, Wangemann P. Epithelial cell stretching and luminal acidification lead to a retarded development of stria vascularis and deafness in mice lacking pendrin. PLoS One. 2011; 6(3):e17949. [PubMed: 21423764]

Lang F, Vallon V, Knipper M, Wangemann P. Functional significance of channels and transporters expressed in the inner ear and kidney. Am J Physiol Cell Physiol. 2007; 293(4):C1187–1208. [PubMed: 17670895]

Levenson MJ, Parisier SC, Jacobs M, Edelstein DR. The large vestibular aqueduct syndrome in children. A review of 12 cases and the description of a new clinical entity. Arch Otolaryngol Head Neck Surg. 1989; 115(1):54–58. [PubMed: 2642380]

Li X, Sanneman JD, Harbidge DG, Zhou F, Ito T, Nelson R, Picard N, Chambrey R, Eladari D, Miesner T, Griffith AJ, Marcus DC, Wangemann P. SLC26A4 targeted to the endolymphatic sac rescues hearing and balance in Slc26a4 mutant mice. PLoS Genet. 2013; 9(7):e1003641. [PubMed: 23874234]

Marcus DC. Characterization of potassium permeability of cochlear duct by perilymphatic perfusion of barium. Am J Physiol. 1984; 247(3 Pt 1):C240–246. [PubMed: 6089576]

Morton CC, Nance WE. Newborn hearing screening--a silent revolution. N Engl J Med. 2006; 354(20):2151–2164. [PubMed: 16707752]

Nakaya K, Harbidge DG, Wangemann P, Schultz BD, Green ED, Wall SM, Marcus DC. Lack of pendrin HCO3- transport elevates vestibular endolymphatic [Ca2+] by inhibition of acid-sensitive TRPV5 and TRPV6 channels. Am J Physiol Renal Physiol. 2007; 292(5):F1314–1321. [PubMed: 17200157]

Ohlemiller KK. Mechanisms and genes in human strial presbycusis from animal models. Brain Res. 2009; 1277:70–83. [PubMed: 19285967]

Ohlemiller KK, Lett JM, Gagnon PM. Cellular correlates of age-related endocochlear potential reduction in a mouse model. Hear Res. 2006; 220(1–2):10–26. [PubMed: 16901664]

Ohlemiller KK, Rice ME, Lett JM, Gagnon PM. Absence of strial melanin coincides with age-associated marginal cell loss and endocochlear potential decline. Hear Res. 2009; 249(1–2):1–14. [PubMed: 19141317]

Royaux IE I, Belyantseva A, Wu T, Kachar B, Everett LA, Marcus DC, Green ED. Localization and Functional Studies of Pendrin in the Mouse Inner Ear Provide Insight About the Etiology of Deafness in Pendred Syndrome. JARO - Journal of the Association for Research in Otolaryngology. 2003; 4(3):394–404. [PubMed: 14690057]

Sadanaga M, Morimitsu T. Development of endocochlear potential and its negative component in mouse cochlea. Hear Res. 1995; 89(1–2):155–161. [PubMed: 8600121]

Shen Z, Marcus DC, Sunose H, Chiba T, Wangemann P. I(sK) Channel in Strial Marginal Cells. Voltage-Dependence, Ion-Selectivity, Inhibition by 293B and Sensitivity to Clofilium. 1997; 3(3): 215–230.

Singh R, Wangemann P. Free radical stress-mediated loss of Kcnj10 protein expression in stria vascularis contributes to deafness in Pendred syndrome mouse model. Am J Physiol Renal Physiol. 2008; 294(1):F139–148. [PubMed: 17959752]

Thalmann R, Miyoshi T, Thalmann I. The influence of ischemia upon the energy reserves of inner ear tissues. Laryngoscope. 1972; 82(12):2249–2272. [PubMed: 4539701]

Viberg A, Canlon B. The guide to plotting a cochleogram. Hear Res. 2004; 197(1–2):1–10. [PubMed: 15504598]

Wangemann P, Itza EM, Albrecht B, Wu T, Jabba SV, Maganti RJ, Lee JH, Everett LA, Wall SM, Royaux IE, Green ED, Marcus DC. Loss of KCNJ10 protein expression abolishes endocochlear potential and causes deafness in Pendred syndrome mouse model. BMC Med. 2004; 2:30. [PubMed: 15320950]

Wangemann P, Liu J, Marcus DC. Ion transport mechanisms responsible for K+ secretion and the transepithelial voltage across marginal cells of stria vascularis in vitro. Hear Res. 1995; 84(1–2): 19–29. [PubMed: 7642451]

Wangemann P, Nakaya K, Wu T, Maganti RJ, Itza EM, Sanneman JD, Harbidge DG, Billings S, Marcus DC. Loss of cochlear HCO3- secretion causes deafness via endolymphatic acidification and inhibition of Ca2+ reabsorption in a Pendred syndrome mouse model. Am J Physiol Renal Physiol. 2007; 292(5):F1345–1353. [PubMed: 17299139]

Zhang W, Dai M, Fridberger A, Hassan A, Degagne J, Neng L, Zhang F, He W, Ren T, Trune D, Auer M, Shi X. Perivascular-resident macrophage-like melanocytes in the inner ear are essential for the integrity of the intrastrial fluid-blood barrier. Proc Natl Acad Sci U S A. 2012; 109(26):10388–10393. [PubMed: 22689949]

Highlights

- *SLC26A4* mutations can cause fluctuating and progressive hearing loss in humans.
- *Slc26a4*-insufficient mice have irreversible hearing loss after 6 months of age.
- Stria vascularis degeneration underlies hearing loss in *Slc26a4*-insufficient ears.
- *Slc26a4*-insufficient mice may be used to study primary strial presbycusis.

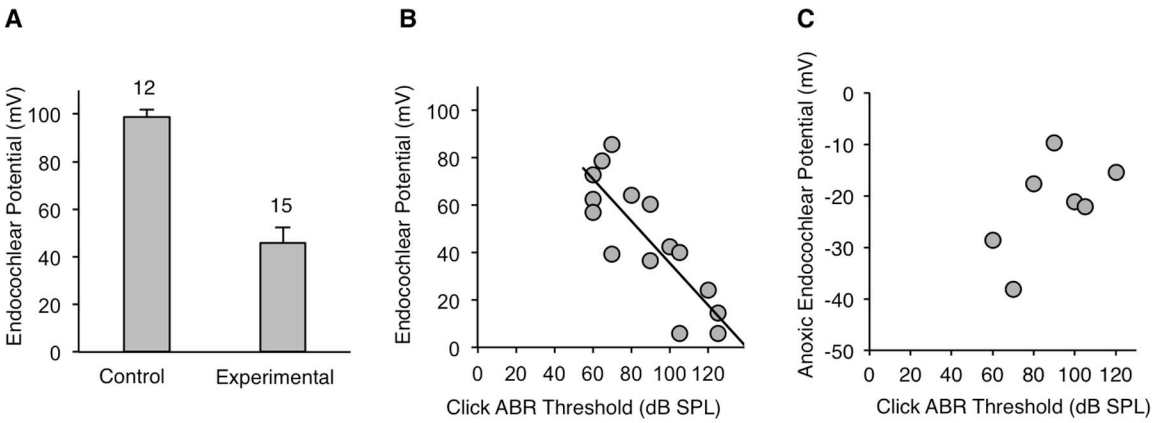

Figure 1.

Auditory function. (A) Endocochlear potential measured at 12 months of age. (B) Endocochlear potential values were inversely correlated with click ABR thresholds measured at 12 months of age ($R = -0.74$, $p < 0.001$). (C) Anoxic endocochlear potential at 12 months of age. Anoxic endocochlear potential values were not correlated with click ABR thresholds ($p=0.17$).

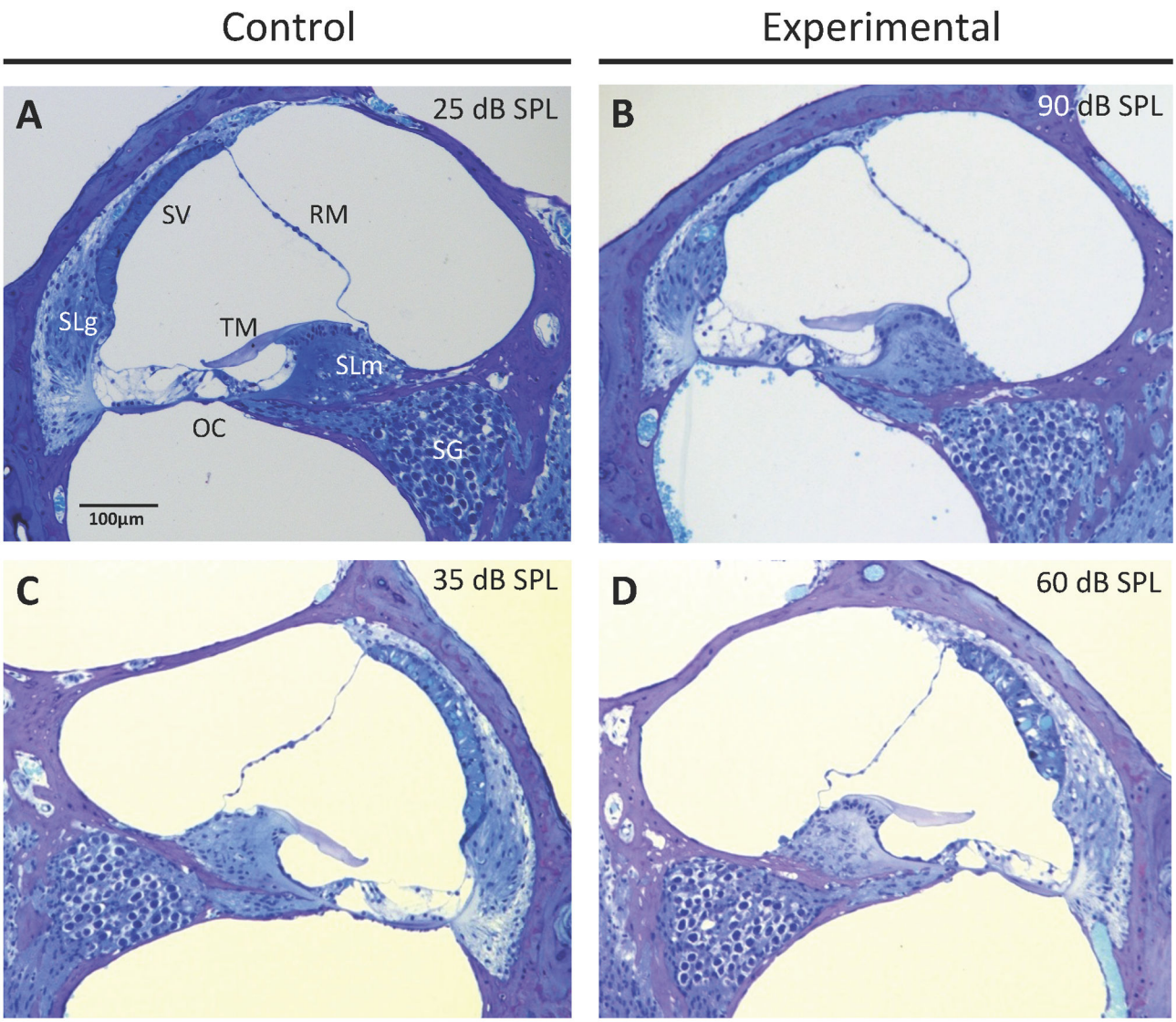

Figure 2.

Cochlear duct histomorphology. Light microscopic images of positive control (A, C) and experimental (B, D) mice at 12 months of age. RM, Reissner's membrane; SV, stria vascularis; SLm, spiral limbus; TM, tectorial membrane; SLg, spiral ligament; OC, organ of Corti; SG, spiral ganglion. Click ABR threshold values for the corresponding ear are shown for each section. (B) Atrophy of the stria vascularis was observed in experimental ears with severe hearing loss. (D) The stria vascularis was edematous in experimental ears with less severe hearing loss.

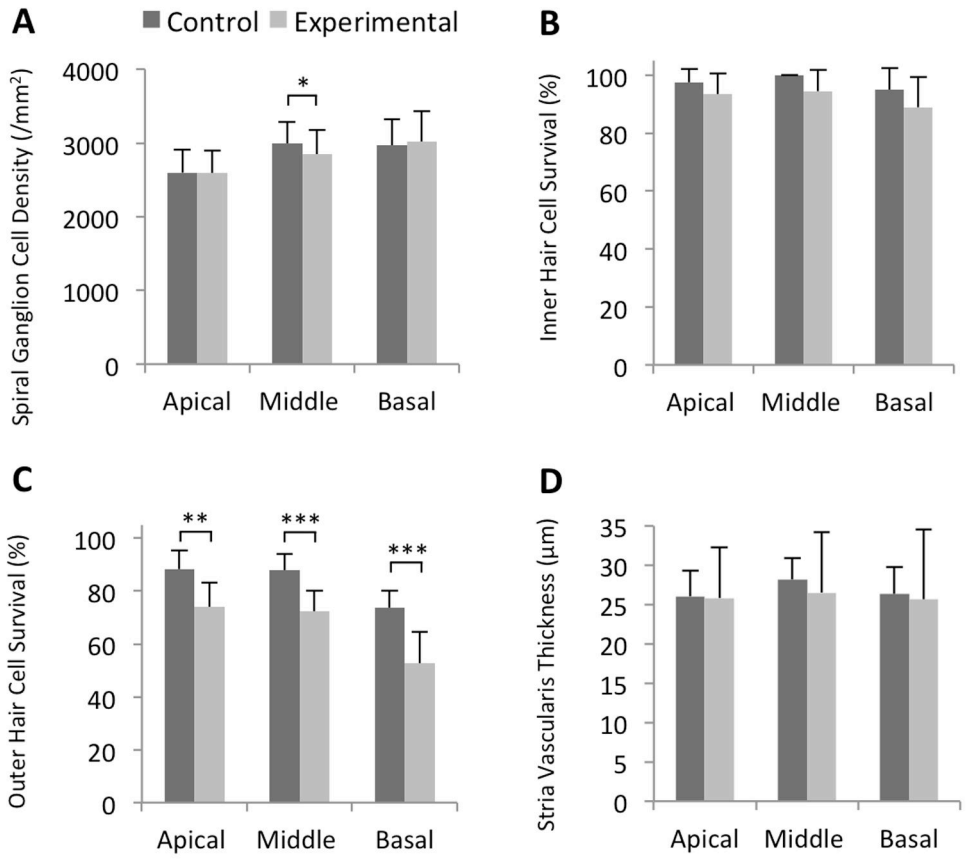

Figure 3.

Measurements of cochlear duct histomorphology. (A) Mean (± S.D.) spiral ganglion cell density, (B) inner hair cell survival rate, (C) outer hair cell survival rate, and (D) stria vascularis thickness. Outer hair cell survival was reduced in all cochlear turns of experimental ears. Spiral ganglion cell density was slightly reduced in the middle turn of experimental cochleae. n = 8 ears for control mice, and n = 9 ears for experimental mice (E, F, G, H). *p = 0.03, **p = 0.003, and ***p < 0.001.

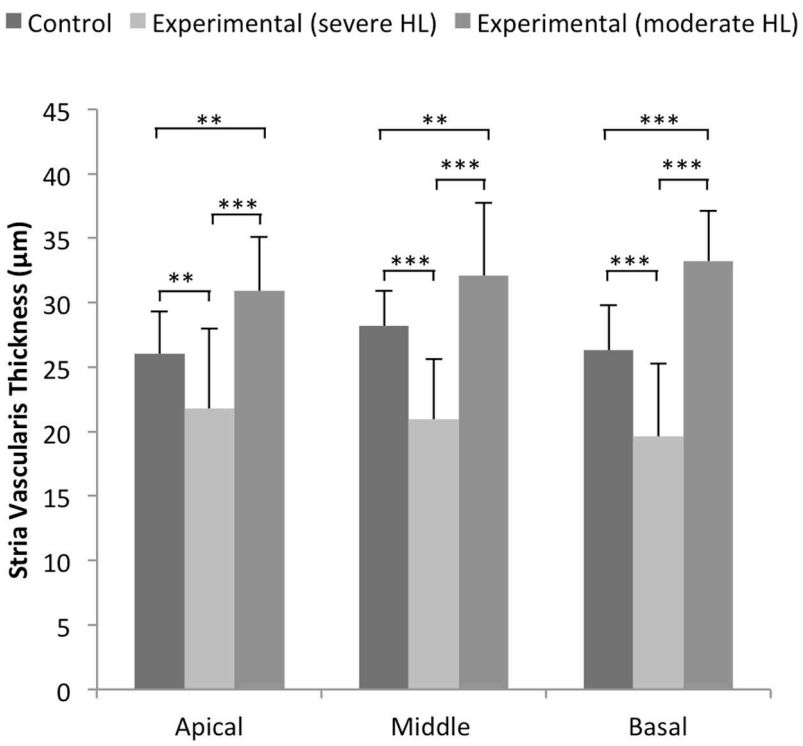

Figure 4.

Stria vascularis thickness and click ABR thresholds. Mean (± S.D.) stria vascularis thickness is shown for 8 control ears, 5 experimental ears with severe hearing loss (HL), and 4 experimental ears with moderate HL. We defined ears with click ABR thresholds ≥80 dB SPL as having severe HL, and ears with <80 dB SPL as having moderate HL. Mean stria vascularis thickness was significantly different among all groups ($p < 0.0001$) in all cochlear turns. Mean stria vascularis thickness of experimental ears with severe HL was smaller than in control ears, and mean stria vascularis thickness of experimental ears with moderate HL was thicker than in control ears in all cochlear turns. **p <0.005 and ***p<0.0001.

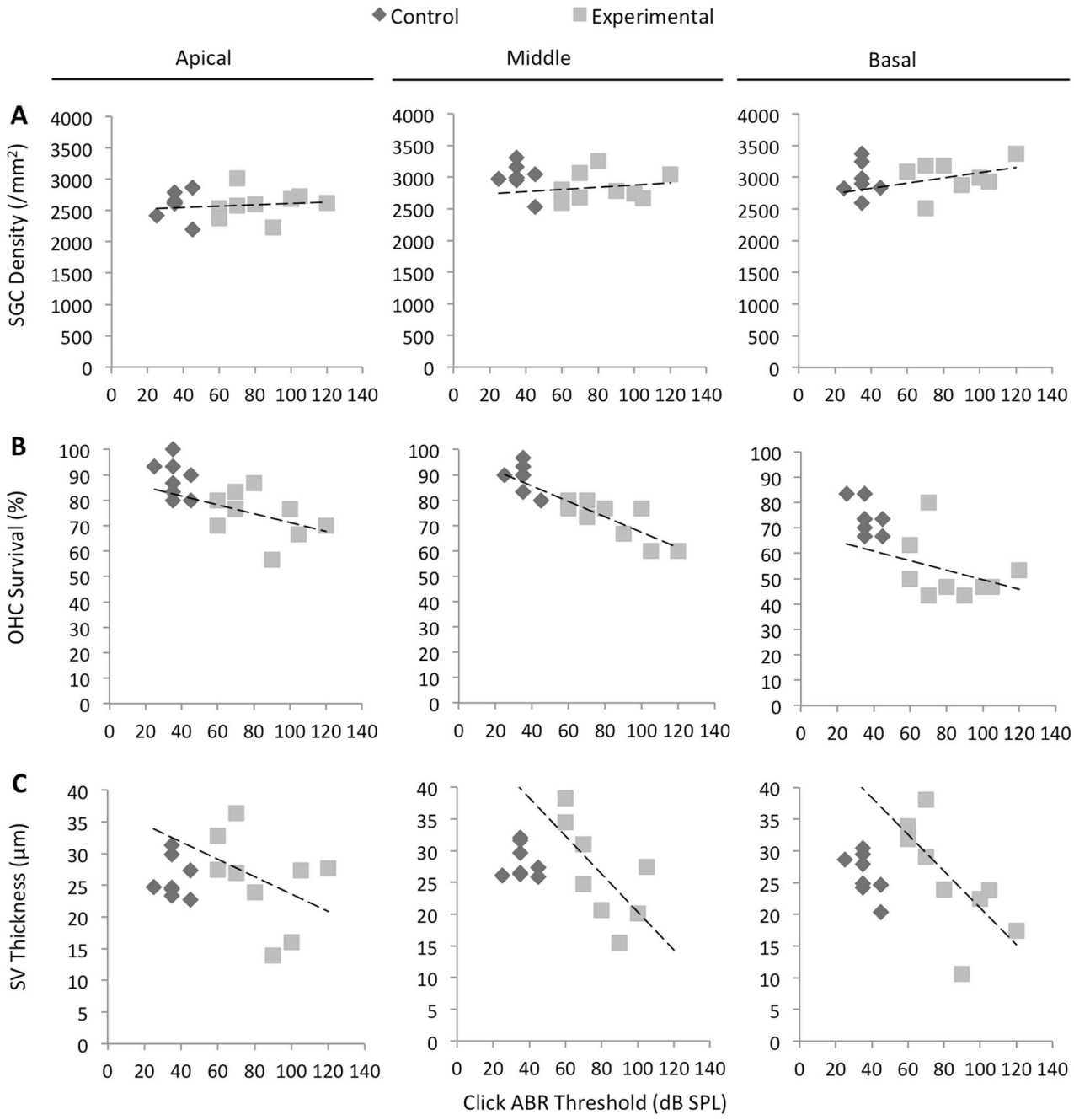

Figure 5.

Correlations of ABR thresholds with cochlear duct histomorphology. n = 8 ears for control mice, and n = 9 ears for experimental mice. Dashed lines represent Pearson correlations for experimental ears. (A) Click ABR thresholds were not correlated with spiral ganglion cell (SGC) density in the apical, middle, or basal turns of experimental cochleae (R = 0.10, p = 0.80; R = 0.16, p = 0.67; and R = 0.32, p = 0.43, respectively). (B) Click ABR thresholds were correlated with outer hair cell (OHC) survival in the middle turn (R = −0.81, p = 0.008) but not in the apical or basal turns of experimental ears (R = −0.40, p = 0.29; and R = −0.33,

p = 0.38, respectively). (C) Click ABR thresholds were correlated with stria vascularis (SV) thickness in the basal turn ($R = -0.72$, $p = 0.03$) but the correlation was not significant in the apical or middle turn ($R = -0.41$, $p = 0.28$; or $R = -0.67$, $p = 0.07$, respectively).

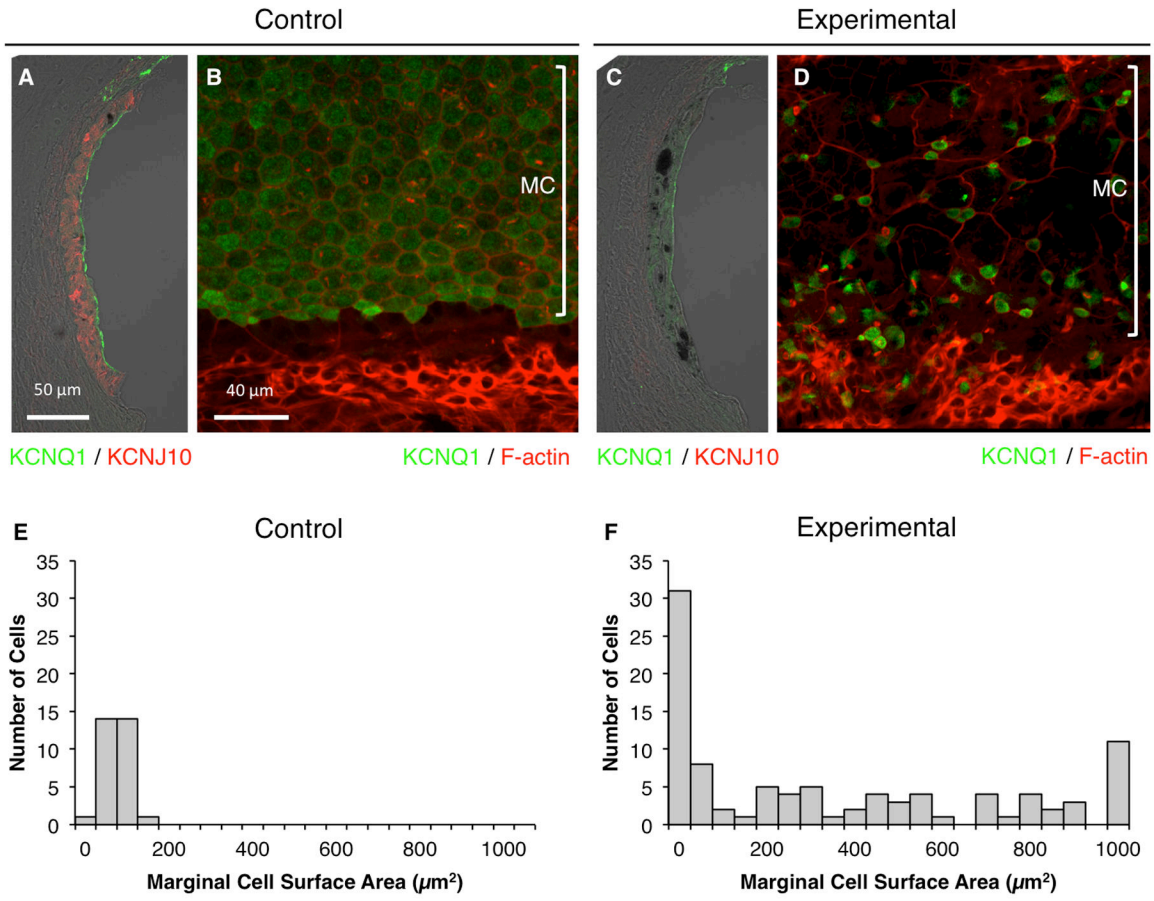

Figure 6.

Stria vascularis protein expression. Representative immunostaining of KCNQ1 (green) and KCNJ10 (red) in cryosections (A, C) or KCNQ1 (green) and F-actin (red) in whole-mounted specimens (B, D) of control (A, B) or experimental stria vascularis (C, D) in the middle turn. n = 6 ears for control mice, and n = 12 ears for experimental mice. MC, marginal cells. KCNQ1 fluorescence was reduced and KCNJ10 staining was absent in experimental ears at 12 months of age. Some marginal cells were expanded and lacked detectable KCNQ1, while others were abnormally small with KCNQ1 concentrated or aggregated within small cell surfaces (D). Apical surface areas of marginal cells for 3 control ears (E; n = 30 cells) and 3 experimental ears (F; n = 96 cells). Bin area = 50 µm^2. If the surface area was > 1050 µm^2, it was included in the 1000–1050 µm^2 bin.

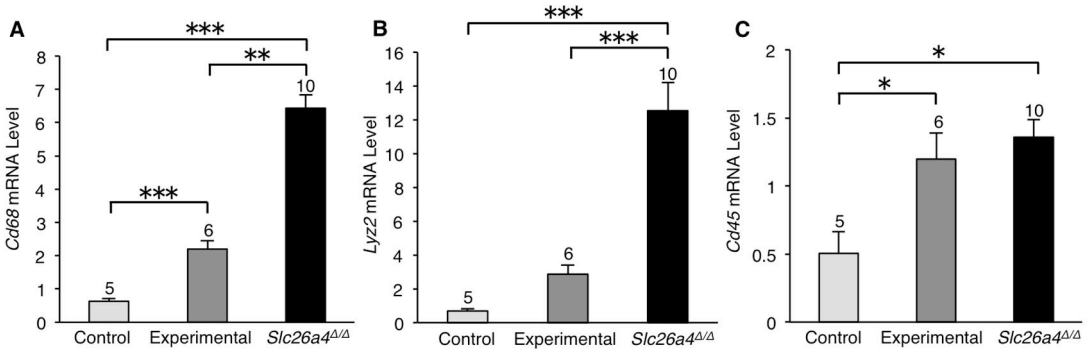

Figure 7.

Expression of macrophage marker genes in stria vascularis. Quantitative RT-PCR analysis was used to measure mRNA levels in stria vascularis from mice at 12 months of age. Data are presented as mean values (± S.E.) of 3 technical replicates for groups of cochleae of each genotype. The number of cochleae used for each genotype group is indicated at the top of each bar. One-way ANOVA was used to identify differences among genotype groups. The mean mRNA levels of *Cd68* (A) and *Cd45* (C) were elevated in experimental striae in comparison to control striae. A similar trend was seen in *Lyz2* mRNA levels (B). Asterisks indicate significant differences: *$p < 0.05$, **$p < 0.01$, and ***$p < 0.005$.

Table 1

Correlations of Click ABR Thresholds with Cochlear Histomorphometry

		Pearson Coefficient R (p value)	
	Cochlear Location	**Control Ears (n = 8)**	**Experimental Ears (n = 9)**
Spiral Ganglion Cell Density	Apical	0.05 (0.90)	0.10 (0.80)
	Middle	−0.39 (0.34)	0.16 (0.67)
	Basal	0.01 (0.98)	0.32 (0.43)
Outer Hair Cell Survival	Apical	−0.36 (0.37)	−0.40 (0.29)
	Middle	−0.65 (0.08)	−0.81 (0.008)*
	Basal	−0.58 (0.13)	−0.33 (0.38)
Stria Vascularis Thickness	Apical	−0.51 (0.90)	−0.41 (0.28)
	Middle	−0.09 (0.84)	−0.67 (0.07)
	Basal	−0.66 (0.08)	−0.72 (0.03)*

*$p < 0.05$